

[Article]

# Multiple Peaks of the Velocity Field as the Linear Perturbations on the Non-Eulerian Inviscid Vortex

TAKAHASHI Koichi

**Abstract** : Stability of the two-dimensional axisymmetric solution for the non-Eulerian inviscid flow governed by the Navier-Stokes equation is analyzed by the linear perturbation method. Two kinds of perturbations are studied. The first one propagates only azimuthally with a constant angular velocity. In the second one, the angular velocity is dependent of radial coordinate. The feature of the latter kind is prominently manifested as the propagation of the turbulence not only to the azimuthal direction but also to the radial direction. In such a mode, the motion of turbulence can take various patterns between two extrema. In one pattern, turbulence propagates inward, disappear, then appear again and propagate outward. In the other one, turbulence propagates inward and completely disappears. Compressibility is the necessary condition for the propagation of turbulences. The result of the present analysis provides a model for understanding the generation and propagation of the second peak of the wind frequently observed in large typhoons.

**Key words** : Navier-Stokes equation ; Euler equation ; inviscid flow ; perturbation ; typhoon

## 1. Introduction

A new solution to the Navier-Stokes equation was recently found by Takahashi (2013). It describes a two-dimensional concentric flow around an axis in inviscid limit. Since it is not derived from the Euler equation, we shall call such a flow non-Eulerian inviscid vortex (NEIV). This flow is maintained through a balance of the centrifugal force and the pressure gradient. The qualitative consistency of its flow profile and the phenomenology of typhoon has also been observed.

In the previous work, it was explored what kinds of perturbations are allowed to the solution. The analysis was done by ignoring the effect of density and pressure perturbations with a result that a prominent peak appears in the azimuthal flow profile and propagated along radial direction. The purpose of the present paper is to take account of the pressure gradient term to evaluate the temporal profile of the full perturbation that includes the contributions from density and pressure.

In some cases, the stability of solution of differential equations is explored by restricting the per-

turbed solution to lay on the surfaces determined by constants of motion. This is particularly effective to investigate the sensitivity of isolated system to the initial conditions (Arnol'd 1965a, b). That is, if the initial state is at the minimum (or, extremum) point of energy on a surface of other constants of motion, the perturbation cannot grow by itself and the state is expected to be stable. Possibility of such stable flows in two-dimension was argued by Vallis et al. (1989). On the contrary, in this paper, our NEIV is assumed to model a large scale motion of atmosphere that always interacts with its environments and thus no constraints other than the equation of motion and the continuity equation are imposed on the perturbation. In particular, energy and enstrophy will not be conserved because they are quadratic in the velocity field. On the other hand, the periodic boundary condition around the symmetry axis will ensure the conservation of circulation that is linear in velocity field.

As the flow is inviscid, the perturbation is governed by the Euler equation, which, together with the continuity equation, is a first order differential equation. This situation will bring about a great simplicity in our investigation. The method is applicable to any 2D concentric flows.

In the next section, the perturbation on the Navier-Stokes equation with a constant angular velocity is studied. In sec.3, the continuity equation and the equation of state are taken into consideration. In sec.4, a case is studied in which the angular velocity of perturbation is coordinate-dependent. A summary is given in sec.5.

## 2. Pressure gradient and perturbation for the flow with a constant angular velocity

### 2.1 Non-Eulerian Inviscid Vortex

The Navier-Stokes equation in cylindrical coordinate is, with obvious notations, the following set of equations :

$$\dot{v}_r + v_r \partial_r v_r + \frac{v_\theta}{r} \partial_\theta v_r + v_z \partial_z v_r - \frac{v_\theta^2}{r} = \nu \left( \nabla^2 v_r - \frac{v_r}{r^2} - \frac{2}{r^2} \partial_\theta v_\theta \right) - \frac{1}{\rho} \partial_r P + f_r, \quad (2.1a)$$

$$\dot{v}_\theta + v_r \partial_r v_\theta + \frac{v_\theta}{r} \partial_\theta v_\theta + v_z \partial_z v_\theta + \frac{v_r v_\theta}{r} = \nu \left( \nabla^2 v_\theta + \frac{2}{r^2} \partial_\theta v_r - \frac{v_\theta}{r^2} \right) - \frac{1}{\rho r} \partial_\theta P + f_\theta, \quad (2.1b)$$

$$\dot{v}_z + v_r \partial_r v_z + \frac{v_\theta}{r} \partial_\theta v_z + v_z \partial_z v_z = \nu \nabla^2 v_z - \frac{1}{\rho} \partial_z P + f_z. \quad (2.1c)$$

The dot denotes partial differentiation in time. The static NEIV solution is obtained for the divergence free field by setting  $v_r = h_1 \ln r / r$ ,  $v_\theta = r^{-1} \int dr r \zeta(r) - h_1 \theta / r$  ( $\zeta$  is the  $z$ -component of the vorticity),  $v_z = 0$  and by taking the limit  $\nu \rightarrow 0$  and  $h_1 \rightarrow 0$  with  $c \equiv -\nu / h_1$  being fixed (Takahashi 2013). In this limit,  $v_\theta$  is dependent on  $r$  only.

For  $v_\theta(r)$ , we shall adopt the solution for an incompressible flow that obeys the equation (Takahashi

2013)

$$v_\theta'' + \frac{\frac{1}{c} \ln r + 1}{r} v_\theta' + \frac{\frac{1}{c} \ln r - \frac{1}{c} - 1}{r^2} v_\theta = 0, \quad (2.2a)$$

The prime stands for a differentiation with respect to  $r$ .  $c$  and  $c_1$  are constant.  $c$  is the ratio of  $\nu$  to the characteristic radial velocity in the course of taking the limit  $\nu \rightarrow 0$ .

(2.2a) can be readily extended to the case in which  $v$  is divergence-free and  $z$ -dependent by preserving the  $z$ -derivative term :

$$\partial_r^2 v_\theta + \frac{\frac{1}{c} \ln r + 1}{r} \partial_z v_\theta + \partial_z^2 v_\theta + \frac{\frac{1}{c} \ln r - \frac{1}{c} - 1}{r^2} v_\theta = 0. \quad (2.2b)$$

However, in this paper, we restrict our considerations to the  $z$ -independent case. In Fig. 1, an example of  $v_\theta(r)$  as a solution of (2.2a) and its derivative is shown.

$v_\theta = 0$  at the center, and stays small around a narrow region around the center.  $v_\theta$  rapidly increases with  $r$  until it reaches a maximum. Then  $v_\theta$  gradually decreases as  $\ln r/r$  at long distances. The width of the peak increases with  $c$ . The behaviour of  $dv_\theta/dr$  near  $r = 0$  clearly shows the existence of an ‘eye’ that resembles that of typhoon. We shall call the maximum in  $v_\theta$  the primary peak.

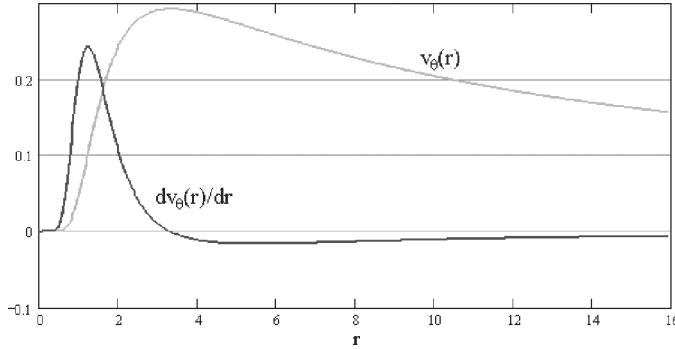


Fig. 1 An example of  $v_\theta(r)$  and  $v_\theta'(r)$  for  $c = 0.1$  and  $c_1 = 1$ . The density  $\rho$  is constant. For the meaning of the parameter  $c$ , see Takahashi (2013).

The well-known Burgers vortex (Burgers 1948) also has the  $v_\theta$ -component only in inviscid limit. The solution presented above differs from the Burgers vortex in that (i) the former has a very small (smaller than any power of  $r$ ) tangential velocity near the symmetry axis while  $v_\theta \propto r$  in the latter and (ii) the circulation at infinity diverges like  $\ln r$  in the former while it is finite in the latter.

The appearance of  $\ln r/r$  term in  $v_\theta$  occurs also in other flows with a special value of the Reynolds number  $Re$ , e.g., a flow of  $Re = -2$  between two rotating cylinders (Hocking 1963) or a flow of  $Re = 2$

with a suction outside a rotating cylinder (Preston 1950).

The NEIV can be regarded as an example of more general non-Eulerian inviscid flow (NEIF). We here give the general definition of the equation that is obeyed by the incompressible NEIF. It reads

$$\lim_{\nu \rightarrow 0} \frac{1}{\nu} \left( \frac{\partial \mathbf{v}}{\partial t} + \mathbf{v} \cdot \nabla \mathbf{v} + \frac{\nabla P}{\rho} - \mathbf{f} \right) = \lim_{\nu \rightarrow 0} \nabla^2 \mathbf{v},$$

where only terms leading in  $\nu$  are retained for each component of  $\mathbf{v}$ . For at least one component, the r.h.s. is required to give non-vanishing contribution. The solution adopted below as the background flow is of a static vortex configuration.

## 2.2 Perturbations

Let us allow small variations of the velocity components as  $v_\theta(r) \rightarrow v_\theta(r) + \delta v_\theta$ ,  $v_r = 0 \rightarrow \delta v_r$ ,  $v_z = 0 \rightarrow \delta v_z$ . At the same time, the pressure and the density are varied as  $P \rightarrow P + \delta P$  and  $\rho \rightarrow \rho + \delta \rho$ , where  $\rho$  is the unperturbed constant density. By substituting these to the original Navier-Stokes equation, we obtain

$$\left( \partial_t + \frac{v_\theta}{r} \partial_\theta \right) \delta v_r - \frac{2v_\theta}{r} \delta v_\theta = -\frac{1}{\rho} \partial_r \delta P + \frac{v_\theta^2}{\rho r} \delta P, \quad (2.3a)$$

$$\left( \partial_t + \frac{v_\theta}{r} \partial_\theta \right) \delta v_\theta + \left( v'_\theta + \frac{v_\theta}{r} \right) \delta v_r = -\frac{1}{\rho r} \partial_\theta \delta P, \quad (2.3b)$$

$$\left( \partial_t + \frac{v_\theta}{r} \partial_\theta \right) \delta v_z = -\frac{1}{\rho} \partial_z \delta P, \quad (2.3c)$$

where the r.h.s.'s of the above equations are, from (2.3a) to (2.3c), the variations of the pressure gradient terms, i.e.,  $-\delta(\partial_r P/\rho)$ ,  $-\delta(\partial_\theta P/\rho)/r$  and  $-\delta(\partial_z P/\rho)$ , respectively. The identities  $\partial_\theta P = 0 = \partial_z P$  and  $\partial_r P/\rho = v_\theta^2/r$ , which hold for the unperturbed flow with  $v_r = v_z = 0$ , have also been used. (2.3a~c) are nothing but the perturbed Euler equation since the viscosity term has been dropped. The perturbation on the external body force has also been assumed to vanish.

The equations are linear in perturbations. Therefore, in the Fourier expansion of physical quantities in the azimuthal angle  $\theta$ , only coupling among the coefficients of a common single mode will take place. Assuming for simplicity that  $\delta v_z$  vanishes and that  $z$ -dependences of physical quantities are absent, we write

$$\delta v_r = A \exp[i(n\theta - \omega t)], \quad (2.4a)$$

$$\delta v_\theta = iB \exp[i(n\theta - \omega t)], \quad (2.4b)$$

$$\delta P = -i\rho C \exp[i(n\theta - \omega t)], \quad (2.4c)$$

$$\delta \rho = i\rho D \exp[i(n\theta - \omega t)]. \quad (2.4d)$$

Here,  $n$  is an integer.  $\omega$  is constant, while the coefficients  $A$ ,  $B$ ,  $C$  and  $D$  may be dependent on

$r$ . The turbulence described by (2.4) propagates azimuthally but not radially because the phase factors are  $r$ -independent.

Substituting (2.4a~d) to (2.3), we have

$$\left(\omega - n \frac{v_\theta}{r}\right)A + \frac{2v_\theta}{r}B = -C' - \frac{v_\theta^2}{r}D, \quad (2.5a)$$

$$\left(v_\theta' + \frac{v_\theta}{r}\right)A + \left(\omega - n \frac{v_\theta}{r}\right)B = -\frac{n}{r}C, \quad (2.5b)$$

where the prime denotes differentiation with respect to  $r$ . Let us choose  $A$  to be real. Then, from (2.5), non-trivial solutions will exist when  $B$  and  $C$  are real.

We here have two equations for four unknown functions. Other equations to be taken into account to determine them may be the continuity equation and the equation of state, about which we are going to discuss in the next section.

### 3. Continuity equation and equation of state

The continuity equation in the first order of perturbation reads

$$\left(\partial_t + \frac{v_\theta}{r}\partial_\theta\right)\delta\rho + \rho\left(\frac{1}{r}\delta v_r + \partial_r\delta v_r\right) + \frac{\rho}{r}\partial_\theta\delta v_\theta = 0. \quad (3.1)$$

Using the expressions (2.4a), (2.4b) and (2.4d) for  $\delta v_r$ ,  $\delta v_\theta$  and  $\delta\rho$ , we have

$$rA' + A - nB + r\left(\omega - n \frac{v_\theta}{r}\right)D = 0. \quad (3.2)$$

The equation of state reflects the thermodynamical property of the system. For example, for an adiabatic change,  $\delta\rho \propto P^{-1+1/\gamma}\delta P$  will hold within linear perturbation. If  $P$  is slowly varying as compared to the perturbations, the proportionality of  $\delta\rho$  and  $\delta P$  may be a good approximation. Thus, it is suggested that

$$D = -\alpha C, \quad (3.3)$$

with a constant  $\alpha$ .  $\alpha = 0$  implies incompressible fluid (2.5a), (2.5b) and (3.2) under the condition (3.3) are the set of equations to be solved. Eliminating  $B$  by using (3.2), the equations (2.5a) and (2.5b) are rewritten for a vector  $\mathbf{V}^T \equiv (A, C)$  as :

$$\frac{d}{dr}\mathbf{V} = \mathbf{M}\mathbf{V}, \quad (3.4)$$

where the ( $r$ -dependent) adjoint matrix  $\mathbf{M}$  is defined by

$$\mathbf{M} = \begin{pmatrix} -\frac{nv_\theta' + \omega}{r\bar{\omega}} & -\frac{n^2}{r^2\bar{\omega}} + \alpha r\bar{\omega} \\ -\bar{\omega} + \frac{2v_\theta}{r^2} & \frac{rv_\theta' + v_\theta}{\bar{\omega}} + \frac{2nv_\theta}{r^2\bar{\omega}} + \frac{\alpha v_\theta^2}{r} \end{pmatrix}, \quad (3.5)$$

where  $\tilde{\omega} \equiv \omega - nv_\theta/r$ . The point  $(A, C)=(0, 0)$  in the  $A$ - $C$  plane is the fixed point of (3.4). From Fig. 1 we see that, for  $r \sim 0$  or  $r \rightarrow \infty$ , the terms in (3.5) involving  $v_\theta$  are very small as compared to remaining terms and can be neglected. In those regions,  $\mathbf{M}$  can be approximately written as

$$\mathbf{M} \approx \begin{pmatrix} -\frac{1}{r} & -\frac{n^2}{\omega r^2} + \alpha\omega \\ -\omega & 0 \end{pmatrix}. \quad (3.6)$$

$C$  then approximately obeys the equation

$$C'' + \frac{1}{r}C' + \left(\alpha\omega^2 - \frac{n^2}{r^2}\right)C \approx 0. \quad (3.7)$$

The regular solution that does not diverge at  $r=0$  and  $\infty$  exists for  $\alpha > 0$  and, apart from normalization, is given by

$$C(r) \approx J_n(\sqrt{\alpha\omega}r), \quad (3.8)$$

where  $J_n$  is the Bessel function. It should be noted that the perturbation exists in case  $\alpha \neq 0$ , i.e., the fluid is compressible.

Near  $r=0$ ,  $C$  behaves as  $r^n$ . Correspondingly,  $A$  and  $B$  behave as  $r^{n-1}$ . In order for  $\mathbf{M}$  given by (3.5) to be non-singular to yield regular solutions,  $\omega$  must be either positive and sufficiently large or negative. Examples of the solution to (3.4) for  $C$  and  $A$  are shown in Fig. 2. The amplitudes with  $n \geq 1$  generally have a maximum at a finite radius.

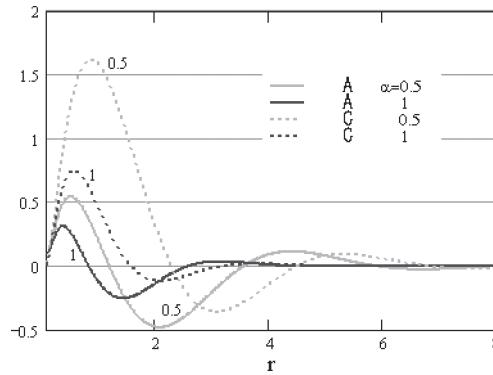


Fig. 2 Examples of the solution for  $A$  and  $C$  with arbitrary unit. Figure on each curve is the value of  $\alpha$ . Parameters are chosen as  $n = 1$ ,  $\omega = -2$ .

#### 4. Differential rotation

In the previous paper (Takahashi 2013), by neglecting the pressure gradient, i.e., r.h.s. of (2.3a) and

(2.3b), the existence of perturbation with non-rigid phase rotation was suggested. In this section, we shall take those pressure gradient terms into consideration to make the previous analysis more accurate.

The perturbations obey the equations (2.3a~c) together with the continuity equation (3.1). Now, we assume that the angular velocity  $\omega$  in (2.4a~d) is  $r$ -dependent, thereby yielding a differential rotation. This assumption emerges from the fact that the time differentiation is always accompanied with the  $r$ -dependent angle-differentiation term. The amplitudes may also be assumed to be  $r$ -dependent and have a common factor  $e^{ikz}$  as e.g.  $\delta v_r = A e^{i(n\theta - \omega(r)t) + ikz}$ ,  $\delta v_\theta = iB e^{i(n\theta - \omega(r)t) + ikz}$ ,  $\delta v_z = iZ e^{i(n\theta - \omega(r)t) + ikz}$  etc. Substituting these to (2.3a~c) and (3.1), we have

$$\left(\omega - n \frac{v_\theta}{r}\right)A + \frac{2v_\theta}{r}B = -C' + i\omega' tC - \frac{v_\theta^2}{r}D, \quad (4.1a)$$

$$\left(\omega - n \frac{v_\theta}{r}\right)B + \left(v_\theta' + \frac{v_\theta}{r}\right)A = -\frac{n}{r}C, \quad (4.1b)$$

$$\left(\omega - n \frac{v_\theta}{r}\right)Z = -kC, \quad (4.1c)$$

$$i\dot{D} + \left(\omega - n \frac{v_\theta}{r}\right)D + \frac{1}{r}A + A' - i\omega' tA - \frac{n}{r}B - kZ = 0. \quad (4.1d)$$

Owing to the appearance of the terms linear in  $t$  in (4.1a) and (4.1d), the density amplitude  $D$  will have a linear-dependence on  $t$  like

$$D = D_0 + iD_1 t. \quad (4.2)$$

Of course, the phase of  $D_1$  must be chosen so as to keep the sign of the density positive. (4.1b~d) show that, when  $A$ ,  $B$ ,  $C$  and  $Z$  are time-independent,  $D_1$  is non-zero only when  $A$  is non-zero. Namely, the radial component of the velocity brings about in- or out-flow of matter and causes the change in density for 2-dimensional flow.

$B$ ,  $C$  and  $Z$  are eliminated to get an equation involving  $A$ ,  $D_0$ ,  $D_1$  and  $\omega$ . Derivation of this equation is given in Appendix. Interestingly, this equation involves only  $A$  and  $\omega$  and expresses that the product of  $A$  with a polynomial of  $\omega$  is zero. When  $A$  is non-zero, this equation leads to an 'eigenvalue' equation for  $\omega$  :

$$\tilde{\omega}^4 - \frac{4v_\theta^2}{r^2}\tilde{\omega}^2 - \frac{4nv_\theta^3}{r^3}\tilde{\omega} - \frac{1}{r^2}\left(\frac{n^2}{r^2} + k^2\right)v_\theta^4 = 0, \quad (4.3)$$

where  $\tilde{\omega}$  has been defined below Eq.(3.5). See Appendix for the derivation of (4.3). When  $k^2$  is real and  $\omega$  is a solution of (4.3), its complex conjugate  $\omega^*$  is also a solution. In addition, (4.3) is invariant under  $n \rightarrow -n$ ,  $\omega \rightarrow -\omega$ . This means that, if  $\omega$  is a solution for an  $n$  then  $-\omega$  is a solution for  $-n$ .

Solutions for special values of  $n$  and  $k$  are given below.

i)  $n=0$  (unstable for  $k \neq 0$ )

$$\tilde{\omega} = \pm \sqrt{2 \pm \sqrt{4 + k^2 r^2}} \frac{v_\theta}{r}. \quad (4.4)$$

ii)  $|n| \rightarrow \infty$  (unstable)

$$\tilde{\omega} \rightarrow \pm \sqrt{\pm n} \frac{v_\theta}{r}. \quad (4.5)$$

iii)  $k=0$  (unstable for  $|n| \geq 2$ )

$$\tilde{\omega} = (1 \pm \sqrt{1+n}) \frac{v_\theta}{r} \text{ or } (-1 \pm \sqrt{1-n}) \frac{v_\theta}{r}. \quad (4.6)$$

Here, a mode of a complex  $\omega$  is called unstable. As is suggested by these extreme cases, the eigenvalue equation (4.3) has both real and complex solutions for almost all regions of parameters. Two complex solutions are mutually complex conjugate. Therefore the perturbation blows up in course of time for one complex solution and decays for the other. The numerical solutions of (4.3) are

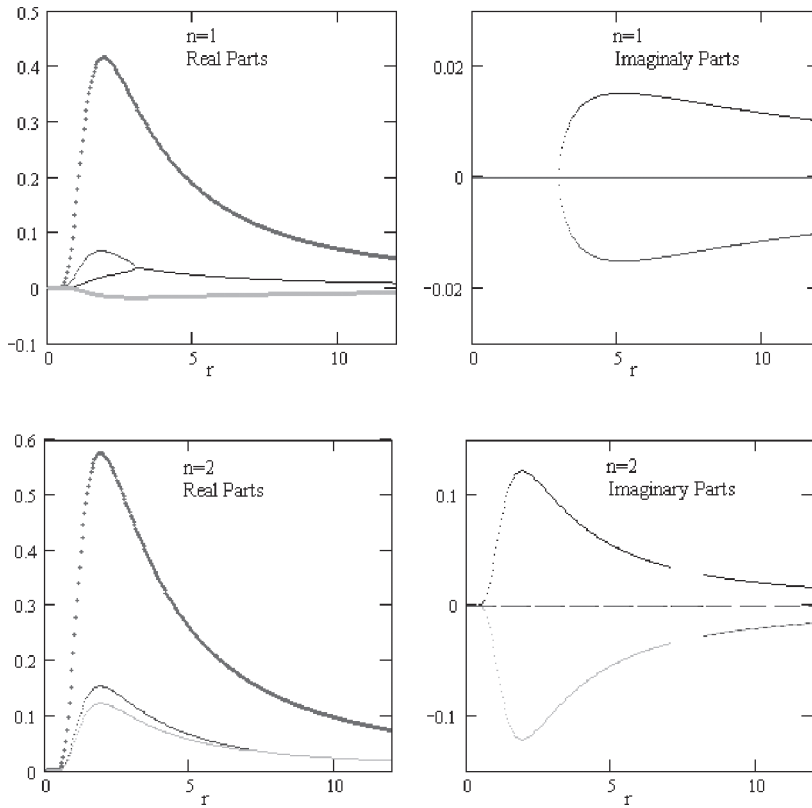


Fig. 3 Real (left) and imaginary (right) parts of four  $\omega$  as functions of  $r$  for  $n=1$ (upper panels) and 2 (lower panels),  $c=0.1$ ,  $k=0.1$ . Two of the  $\omega$ 's are real and the others are complex above the bifurcation point. The bifurcation point is inversely proportional to  $k$ . For  $n=2$ ,  $\omega$ 's with the smallest real part have an imaginary part.



shown in Fig. 3 for  $k_z=0.1$  and  $n=1$  or 2. Errors of a few percent may exist when two branches are contiguous.

Generally, there exist four distinct solutions. The sign of  $n\text{Re}(\omega)$  is positive or negative, corresponding to the mode that propagates positive or negative  $\theta$ -direction, respectively.  $\omega$  with positive imaginary part causes a temporal blow up of the oscillations in velocity field and other physical quantities. The mode with real  $\omega$  is of neutral stability.  $\omega$  with negative imaginary part corresponds to a decaying turbulence. We may call these three modes as growth, stationary and contraction mode, respectively. There exist regions of  $r$  where all frequencies are real. In these regions, four modes can coexist for a long term. It is also noted that the profile of  $\text{Re}\omega$  is similar to that of  $v_\theta$ .

We have seen that the complex  $\omega$ 's are allowed for inviscid flow within linear perturbation where no constraint other than the equations of motion has been imposed on the perturbation. Nevertheless, the concept of NEIV will be a good approximation for real flows of a very large scale like typhoons. Let us assume that, for such flows, the space-dependent complex eigenvalues found above are good approximation for temporal behaviours of perturbations. Now, the system's energy can generally change in accordance with the variations of the velocities, pressure and density. Grow of amplitudes in viscous fluid will require addition of energy. Then, we may expect for viscous flows, when energy is added to the system in any form, the growth modes with  $\text{Im } \omega > 0$  can be excited and the perturbations will grow. When there is no energy supply, the perturbation will decay. In this case the contraction modes with  $\text{Im } \omega \leq 0$  will be of physical ones.

When  $k$  is real, the frequency generally acquires a nonzero imaginary part beyond a certain distance. For surviving decay modes, it is  $r_c=0$  ( $n=0$ ) and  $r_c=3$  ( $n=1$ ) in the above choice of parameters.  $r_c$  decreases as  $k$  increases. When  $k$  is complex,  $\text{Im}(\omega) \neq 0$  in the whole region of  $r$ . We will consider the case of real  $k$  in the followings.

(4.1a~d) and (4.2) are not sufficient to determine the functional form of amplitudes. Instead, the ratios of amplitudes are given by the following relations (See Appendix for derivation) :

$$\frac{B}{A} = \frac{1}{\bar{\omega}} \left( -v'_\theta - \frac{v_\theta}{r} + \frac{n}{\bar{\omega}} \frac{v_\theta^2}{r^2} \right), \quad (4.7)$$

$$\frac{C}{A} = \frac{v_\theta^2}{r\bar{\omega}}, \quad (4.8)$$

$$\frac{Z}{A} = -\frac{k}{\bar{\omega}^2} \frac{v_\theta^2}{r}. \quad (4.9)$$

From equations (4.7)~(4.9), together with the equation (A14) for  $A$ , the  $r$ -dependences of the amplitudes are determined. The case for  $n=0$  is shown in Fig. 4. All of the amplitudes shown here are real and have a peak near  $r=2$ . All of the perturbations are maximized inside the primary peak of

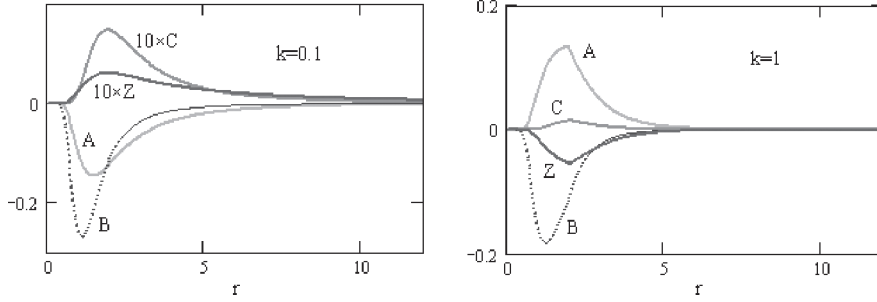


Fig. 4 Perturbation amplitudes  $A$ ,  $B$ ,  $C$  and  $Z$  for real  $\omega$ ,  $n=0$ ,  $k_z=0.1$  (left panel) and 1 (right panel). For  $k=0.1$ ,  $C$  and  $Z$  are magnified by ten-times. The sign of  $A$  is arbitrarily chosen.

$v_\theta$  shown in Fig. 1.

Since  $v_r$  and  $v_z$  are zero for the unperturbed flow, the amplitudes  $A$  and  $Z$  are the direct measures of the corresponding total (i.e., perturbed) velocity components. The  $r$ -dependences of  $\delta v_r$  and  $\delta v_z$  determined by the amplitudes shown in Fig. 5 are shown in Fig. 6. The result for  $k_z=1$  are also shown in the same figure. The direction of the flow changes drastically in the course of time. Simultaneous existence of  $\delta v_r$  and  $\delta v_z$  is a consequence of mass conservation in case no singularity is present (Deppermen 1947).

In order to see the full profile of turbulences, we need to know the  $r$ -dependences of the amplitudes

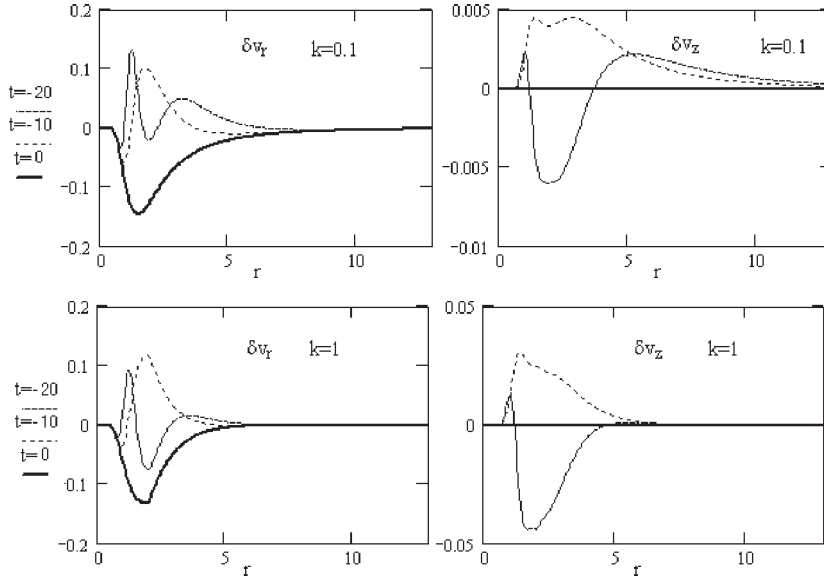


Fig. 5 Perturbed  $\delta v_r$  (upper left) and  $\delta v_z$  (upper right) derived from the amplitudes shown in Fig. 5. Three curves are the velocity profiles at  $t = -20$  (thin solid curve),  $-10$  (dotted curve) and  $0$  (thick solid curve). The lower left and lower right panels are velocity components for  $k_z=1$ .

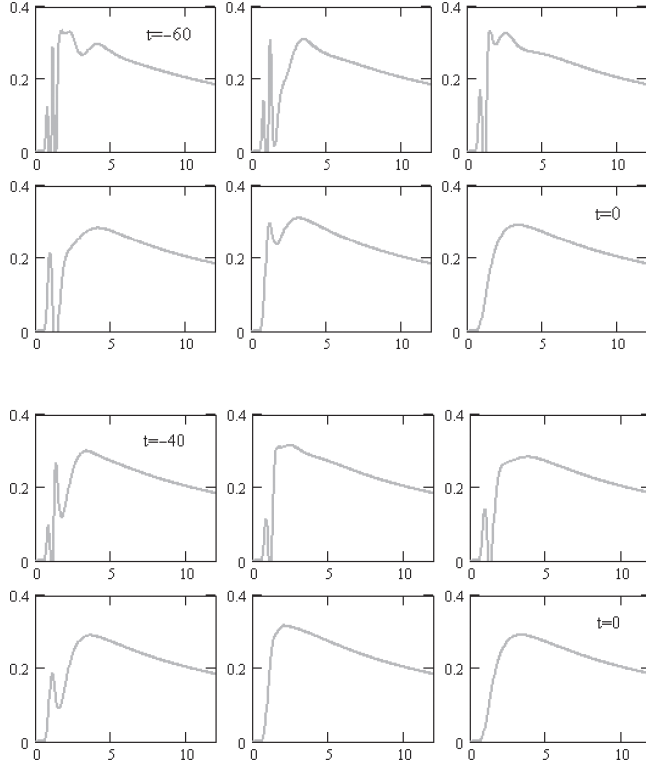


Fig. 6 Upper two rows : An example of the temporal variation of  $v_{\theta, \text{tot}}$  given by (4.9) from  $t = -60$  to 0 (from top left to bottom right; from left to right) for  $n = 0$ ,  $k = 0.1$ ,  $c = 0.1$ ,  $\theta = 0$ ,  $z = 0$ . Amplitude was chosen arbitrarily. Lower two rows :  $k = 1$ ; from  $t = -40$  to 0. Other parameters are same as the upper two rows.

$A$ ,  $B$  etc. This will be achieved by exploiting, e.g., the equation of state that relates  $D_0$  in (4.2) to  $C$  and solving the equations (4.1). Then, e.g. for  $v_\theta$ , the following single-mode perturbation is utilized to observe the total circular flow profile :

$$v_{\theta, \text{tot}} = v_\theta + \text{Re} \left[ i B e^{i(n\theta + kz - \omega t)} \right]. \quad (4.10)$$

Other components are expressed in a similar way.

The immediate conclusion derived from (4.10) is that the turbulences propagate with the phase velocity given by

$$\left( -\frac{\text{Re}(\omega)}{t \text{Re}(\omega')}, \frac{r \text{Re}(\omega)}{n}, \frac{\text{Re}(\omega)}{\text{Re}(k)} \right). \quad (4.11)$$

The radial phase velocity does not have a unique definition. Here in (4.11), the radial component has been defined by a condition  $\text{Re}(\omega)t$  be temporary constant. The  $n = 0$  mode does not propagate in azimuthal direction. The above result implies that the turbulences can in principle propagate to any directions, depending on the signs of  $\text{Re}(\omega)$ ,  $n$  and  $\text{Re}(k)$ . In particular, the radial component is negative for  $t < 0$  and positive for  $t > 0$ . Since the profile of  $\text{Re}(\omega)$  is similar to that of the azimuthal

component, this means that the secondary peak moves first inward and later outward in the outer region. In the core, the motion is opposite. In contrast to the Rossby wave, the direction of the phase velocity is not affected by the Coriolis force.

In the calculations below, the amplitude  $A$  is chosen as a solution of (A14) with  $D_0=0$  for convenience. An example of the temporal behaviour of  $v_{\theta, \text{tot}}$  at  $\theta=0$  is shown in Fig. 6 for  $n=0$ ,  $k=0.1$ . Here a real  $\omega$  has been chosen. At fixed time, several peaks appear due to the factor  $e^{-i\omega(r)}$ . The number of peaks is greater for larger maximum of  $\omega(r)$ . As was expected, the peaks in the region  $\omega' < 0$  move inward when  $t < 0$ . Oppositely those in the region  $\omega' > 0$  move outward. In other words, the perturbation climbs up the slope of  $v_\theta$ . The perturbation climbs down the slope of  $v_\theta$  when  $t > 0$ . The case of  $k=1$  is also shown in Fig. 6.

In Fig. 6, more than one peak existed initially. For smaller  $k$ , the profile of peaks of  $v_\theta$  is finer. The outer peaks moves inward in course of time and disappear at  $t=0$ . Since  $n=0$ , the modulation at  $\theta=\pi$  from the unperturbed  $v_\theta$  is in-phase with that of  $\theta=0$ . In the case of  $k=0.1$ , a fine structure is observed as compared with the case of  $k=1$ . Weakening and intensifying are taking place alternately at a fixed point.

An example of  $n=1$  and  $\text{Im} \omega \leq 0$  is shown in Fig. 7.  $\text{Im} \omega$  is nonzero for  $r > 3$  (see Fig. 3). It is observed that initially one prominent secondary peak is present at around  $r=7$  and moves inward until it merges with the primary peak. During this change, the heights of the peaks get lower.

The difference between the two cases shown respectively in Fig. 6 and Fig. 7 is that, for  $n=0$ ,  $\omega$  is real and the motion at fixed  $r$  is periodic in time thereby yielding the same profiles repeatedly, while, for  $n=1$  ( $r_c=3$ ),  $\text{Im} \omega$  is negative in the region  $r > r_c$  and the initial turbulences located beyond  $r_c$  decay exponentially. Although not shown here, after  $t=0$ , the turbulences substantially disappear beyond the primary peak of  $v_\theta$ . Even in this case, small turbulences generally remain and periodically repeat the appearance and disappearance in the region where  $\text{Im}(\omega)$  is zero. The region where the turbulence is observed for a long time span diminishes as  $k$  gets larger. The long-time turbulence is further suppressed for complex  $k$ .

As was mentioned before, the turbulence around the NEIV does not conserve but increases the energy. Thus an input of energy is a requisite for the excitation of the growth mode, which should be followed by the stationary and contraction modes after cutting off the supply of energy.

Two three-dimensional flow profiles are shown in Fig. 8. A concentric structure and a spiral structure of the eye wall are clearly observed in the mode  $n=0$  and 1, respectively. Also in the latter case, the double wall is observed in almost all radial directions.

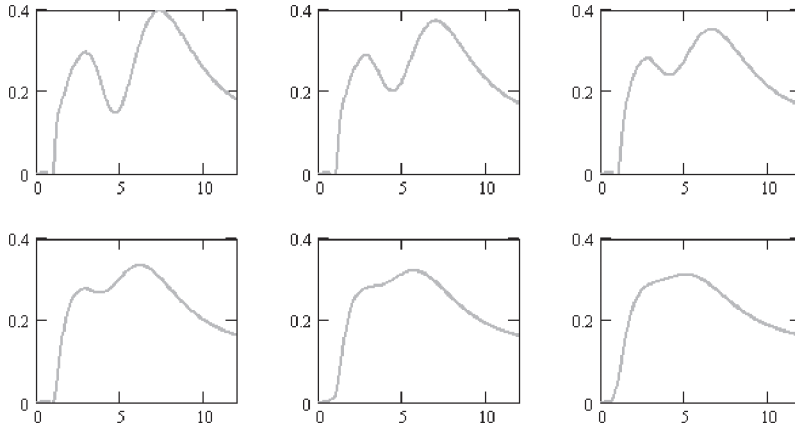


Fig. 7 An example of the temporal variation of  $v_{\theta, tot}$  given by (4.9) from  $t = -60$  to  $0$  with equal time intervals (from top left to bottom right ; from left to right) for  $n = 1, k = 0.1, c = 0.1, \theta = 0, z = 0$  and for a certain choice of amplitude.

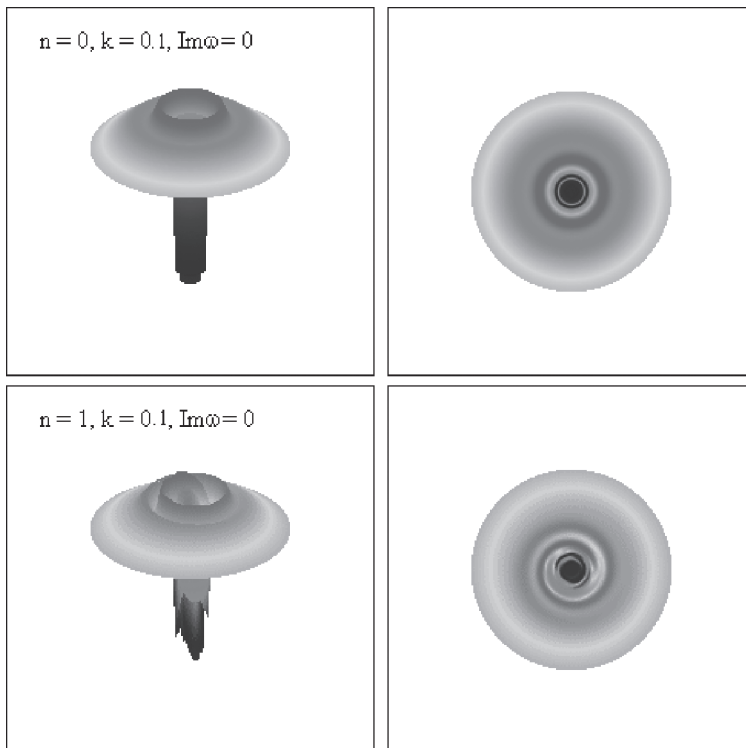


Fig. 8 Three-dimensional flow profiles  $v_{\theta, tot}$  for  $r < 9$  at  $t = -50$ . Left : bird's eye view, Right : view from a point on the polar axis. Model parameters for upper panels :  $n=0, k=0.1$  and for lower panels :  $n=1, k=0.1$ . Unit for the vertical axis is arbitrary.

## 5. Summary and remarks

In this paper, two kinds of perturbations around the axisymmetric NEIV are considered. In the perturbation of the first kind, turbulences of the flow velocity, the pressure and the density are periodic in  $\theta$  and  $t$ . They propagate azimuthally but not radially. The angular velocity of the azimuthal propagation is real and constant. Turbulence rotates as if it were a rigid body. Obviously, this kind of perturbations must be of a small spatial scale.

In the perturbation of the second kind, the angular velocity is generally complex and is a function of the radial coordinate, thereby rendering the temporal behaviour aperiodic. The gross  $r$ -dependence of the angular momentum is similar to that of  $v_\theta(r)$ . Thus, this kind of perturbations can be of a large scale. Together with relatively high oscillations in radial direction, there can appear a prominent peak of turbulence beyond the primary maximum of  $v_\theta$ . With the lapse of time, it moves inward and disappears if the imaginary part of the angular momentum is negative. On account of the requisite compressibility, both kinds of perturbation are of the density waves.

These results based on (3.4) and (4.3) do not depend on the functional form of the concentric flow,  $v_\theta(r)$ .

It seems worthwhile to notice a striking similarity of the starting flow solution to the typhoon models. Our analysis is based on the NEIV generated by barotropic balance. There  $v_\theta(r)$  is very small near the symmetry axis, rapidly increases with  $r$ , takes a maximum at a certain radius and then monotonically decreases to zero as  $\ln r/r$ . This behaviour of the azimuthal velocity is similar to the horizontal wind profiles of the typhoon models (Fujita 1952, Holland 1980, Merrill 1984, DeMaria 1987, Emanuel 2004, Holland et al. 2010) developed from the modified Rankine vortex model (Hughes 1952). The distinctive features of our  $v_\theta(r)$  is that it has an ‘eye’ at the center and exhibits non-power decay at long distances, which is also in agreement with the observations. This indicates that the thermally averaged intermediate level profile of typhoon can be understood in terms of the Newtonian mechanics. It is known that the track of typhoon predicted by a model calculation is sensitive to the form of  $v_\theta(r)$  (Holland and Leslie 1995). Utilizing the flow profile given by  $v_\theta$  in the calculation of typhoon track will be intriguing.

Unfortunately, the perturbations  $\delta v_r$  and  $\delta v_z$  obtained in the previous sections are strongly oscillating in time and do not reproduce observations on real typhoon. In reality,  $\delta v_r$  is negative and  $|\delta v_r|$  is an increasing function of  $r$  outside the primary peak of  $v_\theta$  where a convection ring exists (Depperman 1947). At the convection ring, steady updraft has been observed at intermediate levels in the typhoon

wind, which is of course constrained of having zero upward velocity at the sea surface. Thus it will be worthwhile to explore what occurs to  $\delta v_r$  and  $\delta v_z$  if physically meaningful boundary conditions are taken into account, which is an entirely non-trivial problem because  $\omega$  is complex, albeit non-vanishing  $\delta v_r$  and  $\delta v_z$  are also a consequence of temperature difference between the core and environments in real typhoon (Depperman 1947). Namely, in our scheme of purely Newtonian dynamics (i.e., no thermodynamical effects being taken into account), one may envisage the system to be closed downward and be open upward. Then, the existences of flow in inward radial direction and the peak in  $v_\theta$  at some radius, together with the continuity, will solely imply an emergence of a convective ring.

It is also notable that real typhoons sometimes exhibit the second peak (and in some cases, the third peak, too) of  $v_\theta(r)$ . There are many hypotheses proposed so far to explain the formation of the secondary eyewall (See e.g., Terwey and Montgomery 2008). One of the characteristic of the secondary eyewall is its inward movement (see e.g., Willoughby et al. 1989). Such a behaviour of turbulence might be interpreted as the perturbation of the second kind discussed in this paper, provided that the secondary peak is associated with a strong upflow under realistic boundary conditions. Willoughby et al. (1989) reported that the region of turbulence formed a circle or semicircle. In our terminology, this phenomenon is interpreted that the mode of  $n = 0$  or 1 dominated. Higher modes will possibly be excited, too.

It should be kept in mind that, in reality, the formation and movement of the second peak in azimuthal velocity occur through the life cycle of typhoon. In particular, the merge of two peaks seems to mark the period of transition from typhoon to tropical cyclone. In our view, this process will correspond to the complex  $\omega$  with a negative imaginary part. Confirming further the applicability of our model to the real typhoon will require analyses that take account of the variations of such model parameters as  $c$  and  $c_1$  as well as the superposition of modes that fulfill given boundary conditions.

The perturbation associated with a vortex of a planetary scale has been known as the Rossby wave. The essential point of the emergence of this wave is the interaction of the vorticity with the rotation of the earth. The phase velocity of the Rossby wave is determined through the relation of the background flow with the Coriolis force. In contrast, the perturbations we explored in the present paper do not depend on the Coriolis force and propagate to any directions with the space-time dependent velocity determined by the background velocity field together with the mode. Future advance in observation will enable to judge the existence of the wave of this kind in typhoons or hurricanes.

**Appendix : Eigenfrequency equation**

In this Appendix, starting from (4.1) and (4.2) in the main text, the equation is derived that determines the  $r$ -dependence of the frequency  $\omega$ . Note that explicitly  $t$ -dependent terms exist in (4.1a) and (4.1d). These terms must be cancelled by similar  $t$ -dependent terms involved in  $D$ . Then this kind of cancellations take place when

$$\omega' C - \frac{v_\theta^2}{r} D_1 = 0, \quad (\text{A1})$$

$$\tilde{\omega} D_1 - \omega' A = 0, \quad (\text{A2})$$

where  $\tilde{\omega} \equiv \omega - nv_\theta/r$ . By comparing  $t^0$  terms in (4.1a~d), we obtain

$$\tilde{\omega} A + \frac{2v_\theta}{r} B = -C' - \frac{v_\theta^2}{r} D_0, \quad (\text{A3})$$

$$\tilde{\omega} B + \left(v_\theta' + \frac{v_\theta}{r}\right) A = -\frac{n}{r} C, \quad (\text{A4})$$

$$\tilde{\omega} Z = kC, \quad (\text{A5})$$

$$D_1 - \tilde{\omega} D_0 - \frac{1}{r} A - A' + \frac{n}{r} B + kZ = 0. \quad (\text{A6})$$

Eliminating  $D_1$  from (A1) and (A2), we have

$$\tilde{\omega} C - \frac{v_\theta^2}{r} A = 0. \quad (\text{A7})$$

(A6), (A3) and (A1) form the set of differential equations

$$A' = -\frac{1}{r} A + \frac{n}{r} B + D_1 - \tilde{\omega} D_0 + \frac{k^2}{\tilde{\omega}} C, \quad (\text{A8})$$

$$C' = -\tilde{\omega} A - \frac{2v_\theta}{r} B - \frac{v_\theta^2}{r} D_0, \quad (\text{A9})$$

$$\tilde{\omega}' = \tilde{\omega} \frac{D_1}{A} - n \left( \frac{v_\theta}{r} \right)', \quad (\text{A10})$$

where (A5) has been used to eliminate  $Z$ . Remaining equations (A4) and (A7) are the constraints that are used to express  $B$  and  $C$  in terms of  $A$  :

$$B = -\frac{1}{\tilde{\omega}} \left( v_\theta' + \frac{v_\theta}{r} + \frac{n}{\tilde{\omega}} \frac{v_\theta^2}{r^2} \right) A, \quad (\text{A11})$$

$$C = \frac{v_\theta^2}{r\tilde{\omega}} A. \quad (\text{A12})$$

Dividing both sides of these equations by  $A$ , together with (A.5), we have (4.6), (4.7) and (4.8) in the main text.

Differentiating both sides of (A12) with respect to  $r$  leads to

$$C' = \frac{v_\theta^2}{r\tilde{\omega}} A' + \left( \frac{v_\theta^2}{r\tilde{\omega}} \right)' A. \quad (\text{A13})$$



(A2), (A11) and (A12) can be used to express  $A'$  in (A8) and  $C'$  in (A9) in terms of  $A$  and  $D_0$  as

$$A' = -\left(\frac{1}{r} + \frac{n}{\bar{\omega}}\left(\frac{2v_\theta}{r^2} - \frac{n}{\bar{\omega}}\frac{v_\theta^2}{r^3}\right) - \frac{k^2}{\bar{\omega}^2}\frac{v_\theta^2}{r}\right)A + \frac{\bar{\omega}'}{\bar{\omega}}A - \bar{\omega}D_0, \quad (\text{A14})$$

$$C' = -\left(\bar{\omega} - \frac{2v_\theta}{\bar{\omega}r}\left(v_\theta' + \frac{v_\theta}{r} + \frac{n}{\bar{\omega}}\frac{v_\theta^2}{r^2}\right)\right)A - \frac{v_\theta^2}{r}D_0. \quad (\text{A15})$$

On the other hand, by using (A14), we eliminate  $A'$  in (A13) to obtain

$$C' = \frac{v_\theta^2}{r\bar{\omega}}\left[-\left(\frac{1}{r} + \frac{n}{\bar{\omega}}\left(\frac{2v_\theta}{r^2} - \frac{n}{\bar{\omega}}\frac{v_\theta^2}{r^3}\right) - \frac{k^2}{\bar{\omega}^2}\frac{v_\theta^2}{r}\right)A + \frac{\bar{\omega}'}{\bar{\omega}}A - \bar{\omega}D_0\right] + \left(\frac{v_\theta^2}{r\bar{\omega}}\right)'A. \quad (\text{A16})$$

Equating (A16) to (A15),  $D_0$  disappears and only  $A$  remains. Then, assuming that  $A$  is nonzero, we have the equation (4.3) in the main text.

## References

- Arnol'd V I 1965a : Conditions for nonlinear stability of stationary plane curvilinear flows of ideal fluid. *Dokl. Akad. Nauk, SSSR* **162** 97 [trans. in *Soviet Math.* **6** 773-777 (1965)].
- Arnol'd V I 1965b : Variational principle for three-dimensional steady-state flows of an ideal fluid. *Prikl. Math. I Mech.* **29** 846 [transl. *J. Appl. Math. Mech.* **29** 1002-1008 (1965)].
- Burgers J M 1948 : A mathematical model illustrating the theory of turbulence. *Adv. Appl. Mech.* **1** 171.
- DeMaria M 1987 : Tropical cyclone track prediction with a barotropic spectral model. *Mon. Wea. Rep.* **115** 2346.
- Depperman C E 1947 : Notes on the origin and structure of Philippine typhoon. *Bull. Amer. Meteor. Soc.* **28** 399-404.
- Drazin P and Riley N 2006 : *The Navier-Stokes Equations A Classification of Flows and Exact Solutions* Cambridge Univ. Press (Cambridge).
- Emanuel K A 2004 : Tropical cyclone energetics and structure. *Atmospheric Turbulence and Mesoscale Meteorology*, Federovich E et al (eds) Cambridge Univ. Press (Cambridge), 165-192.
- Fujita T 1952 : Pressure distribution within a typhoon. *Geophys. Mag.* **23** 437-451.
- Hocking L M 1963 : An example of boundary layer formation. *AIAA J.* **1** 1222.
- Holland G J 1980 : An analytic model of the wind and pressure profiles in hurricanes. *Mon. Wea. Rev.* **108** 1212-1218.
- Holland G J and Leslie L M 1995 : On the bogussing of tropical cyclones in numerical models : a comparison of vortex profiles. *Meteorol. Atmos. Phys.* **56** 101-110.
- Holland G J, Belanger J I and Fritz A 2010 : A revised model for radial profiles of hurricane winds. *Mon. Wea. Rep.* **138** 4393 and references cited therein.
- Merrill R T 1984 : A comparison of large and small tropical cyclones *Mon. Wea. Rep.* **112** 1408.
- Preston J H 1950 : The steady circulatory flow about a circular cylinder with uniformly distributed suction at the surface. *Aeronaut Q.* **1** 319.
- Takahashi K 2013 : Vorticity equation, current conservation and the solutions of the Navier-Stokes equation. *Facul. Lib. Arts Rev. (Tohoku Gakuin Univ.)* [www.tohoku-gakuin.ac.jp/research/journal/bk2013/no01.htm](http://www.tohoku-gakuin.ac.jp/research/journal/bk2013/no01.htm)
- Terwey W D and Montgomery M T 2008 : Secondary eyewall formation in two idealized, full-physics modeled hurricanes. *J. Geophys. Res.* **113** D12112.
- Vallis G K, Carnevale G F and Young W R 1989 : Extremal energy properties and construction of stable solutions of the Euler equations. *J. Fluid Mech.* **207** 133.

Willoughby H E, Clos J A and Shoreibah M G 1982 : Concentric eye walls, secondary wind maxima, and the evolution of the hurricane vortex. *J. Atmos. Sci.* **39** 395.